Conditional Probability Estimation for Significant Tornadoes Based on Rapid Update Cycle (RUC) Profiles

WILLIAM E. TOGSTAD

Edina/Minneapolis, Minnesota

JONATHAN M. DAVIES

Trimble/Kansas City, Missouri

SARAH J. CORFIDI

Cooperative Institute for Mesoscale Meteorological Studies, Norman, Oklahoma

DAVID R. BRIGHT

NCEP/AWC, Kansas City, Missouri

ANDREW R. DEAN

NOAA/Storm Prediction Center, Norman, Oklahoma

(Manuscript received 7 May 2010, in final form 28 February 2011)

ABSTRACT

Recent literature has identified several supercell/tornado forecast parameters in common use that are operationally beneficial in assessing environments supportive of supercell tornadoes. These parameters are utilized in the computation of tornado forecast guidance such as the significant tornado parameter (STP), a dimensionless parameter developed at the Storm Prediction Center (SPC) that applies a subjectively chosen scale. The goal of this research is to determine if useful logistic regression equations can be developed to estimate the conditional probability of supercell tornadoes that are categorized as level 2 or stronger on the enhanced Fujita scale (EF) when a similar set of environmental background parameters is applied as variables. A large database of Rapid Update Cycle (RUC) analysis soundings in proximity to a representative sample of tornadic and nontornadic supercells over the central and eastern United States, a number of which were associated with EF2 or stronger tornadoes, was used to compute supercell tornado forecast parameters similar to those in the original version of STP. Three logistic regression equations were developed from this database, two of which are described and analyzed in detail. Statistical verification for both equations was accomplished using independent data from 2008 in proximity to supercell storms identified by staff at SPC. A recent version of the STP was utilized as a comparison diagnostic to accomplish part of the statistical verification. The results of this research suggest that output from both logistic regression equations can provide valuable guidance in a probabilistic sense, when adjustments are made for the ongoing convective mode. Case studies presented also suggest that this guidance can provide information complementary to STP in severe weather situations with potential for supercell tornadoes.

1. Introduction

Remarkable strides have been made over the past two decades in quantifying a variety of convective parameters in common use by both research and operational meteorologists regarding supercell tornadoes. For example, Rasmussen and Blanchard (1998, hereafter RB98) gathered a large database of observed upper-air soundings selected as being representative of inflow conditions for both supercell and nonsupercell thunderstorms. This research found that combinations of individual convective parameters frequently scored higher than their individual

Corresponding author address: William E. Togstad, 4908 Aspasia Ln., Edina, MN 55435-4068.
E-mail: wtogstad@comcast.net

DOI: 10.1175/2011WAF2222440.1

components in terms of effectively discriminating between three classes of thunderstorm environments. In particular, the combination of convective available potential energy (CAPE) and vertical wind shear, utilized in both the energy helicity index (EHI; Hart and Korotky 1991; Davies 1993) and the vorticity generation parameter (VGP; RB98), provided superior discrimination scores compared to various measures of shear or CAPE alone. A follow-up study by Rasmussen (2003, hereafter R03) revealed that use of data from 0 to 1 km above ground layer (AGL) in computing storm-relative helicity (SRH; Davies-Jones et al. 1990) and EHI yielded improved discrimination between populations of tornadic and nontornadic supercells when compared to the 0–3-km AGL depth.

The Rapid Update Cycle (RUC) analysis and forecast system (Benjamin et al. 2004) offers a unique opportunity for dramatically increasing the sample size for thunderstorm environment research by providing high spatial and temporal resolution model estimation soundings in close proximity to thunderstorms. The work of Thompson et al. (2003 and 2007, hereafter T03 and T07, respectively) using RUC model analysis soundings reinforced the findings of R03 that vertical shear and moisture information within the lowest 1 km AGL can discriminate between environments supporting nontornadic supercells and tornadic supercells associated with significant tornadoes [level 2 or greater on the enhanced Fujita scale (EF)]. Davies (2004, hereafter D04) used a similar database of RUC model analysis soundings to demonstrate the general limiting effect that increasing values of mixed layer convective inhibition (MLCIN; Colby 1984) tend to have on tornado frequencies.

Some of the above research has become a springboard for the development of additional multiparameter severe weather composite indices at the Storm Prediction Center (SPC). For example, T03 described and evaluated the performance of both the supercell composite parameter (SCP) and the significant tornado parameter (STP); these parameters are used as guidance for meteorologists tasked with routinely evaluating and monitoring severe weather risk. With additional experience and research, both indices have been updated to account for variations in the thunderstorm inflow layer and the depth of the thunderstorm cloud layer (Thompson et al. 2011, T07).

The main purpose of this research is to explore the possibility that useful logistic regression models might be developed for assessing the conditional probability of significant (EF2 or stronger) tornadoes when environmental background parameters such as those described in earlier work (e.g., T03, R03, D04, T07) are applied as independent variables. It should be noted that because the database utilized for regression equation development was entirely composed of RUC analysis soundings in proximity to observed supercell thunderstorms, the probability output is only valid when a supercell thunderstorm is present.

Some limitations and challenges to the research goal described above are briefly discussed in the following section. In section 3, a review of the development database is provided. A discussion and description of logistic regression equations developed through application of convective parameters extracted from this database follows in section 4. Section 5 provides verification statistics using an independent dataset for 2008 that comprises a variety of descriptive metrics and environmental data for 1695 supercells identified by SPC staff. The operational use of the regression equations along with several brief case examples is contained in section 6, and a concluding discussion is provided in section 7.

2. Limitations on assessing conditional tornado probability from sounding-derived environment parameters

Meteorological research and operational experience suggest a number of obstacles to assessing significant tornado risk solely from synoptic and mesoscale environment parameters. For example, Thompson and Mead (2006) and Thompson et al. (2008) found that significant tornado threat is often greater with discrete convective cells, and the same threat may be reduced if the convection evolves into a linear mode too quickly. However, determining the probable convective mode and its evolution with time on a given day is often very difficult. Dial et al. (2010) developed a methodology for determining the short-term convective mode using the angular orientation of mean winds and vertical shear in layers aloft relative to the low-level boundary initiating thunderstorms. Their findings suggest that any statistical approach may have limited effectiveness without consideration of convective modes.

In addition to this, a number of researchers (e.g., Brooks et al. 1994; Stensrud et al. 1997; T03) provided evidence that tornado development may depend on both the strength of the storm-relative flow at various levels as well as a balance of storm-relative flow between the low and middle levels of the storm. Because of the complexities of predicting storm motion and the resulting storm-relative winds, parameters that incorporate storm-relative flow at different levels have not performed particularly well when compared to other supercell and tornado parameters (e.g., see RB98 and T03).

Finally, there is considerable evidence that subtle differences in hodograph structure and shape in the lowest 1 km of the atmosphere may be very important in

discriminating between tornadic and nontornadic storms (e.g., Markowski et al. 2003). The numerical modeling experiments by Wicker (1996) suggest that a detailed knowledge of the vertical wind shear in the lowest several hundred meters is required for determining the likelihood of low-level mesocyclogenesis. Thompson and Edwards (2000), Miller (2006), and Esterheld and Giuliano (2008*)* provide observational evidence of the importance of hodograph shape and structure in the lowest 500 m AGL for a number of significant tornado events. Such hodograph details are difficult (if not impossible) to incorporate into a statistical approach involving environment parameters that provide only a single ''number'' as output for reference.

To summarize, because the logistic regression models described in this paper are based on a limited number of environmental background parameters, application of these statistical results will not provide any ''magic bullet'' in terms of discriminating between significant tornadoes or weak tornadoes associated with supercells. Nevertheless, because the statistical relations are based on findings from prior tornado environment studies and represent relevant physical processes, useful information may be derived if a skillful mesoanalyst or warning forecaster utilizes them intelligently. Because the statistical relations formulated and examined in this study yield conditional probabilities rather than a parameter or ''index'' value, they may also provide added utility for severe weather forecasters because uncertainty is directly quantified. A quantification of uncertainty should be included in all forecasts (NRC 2006).

3. Convective parameter database

The RUC database used for the development of conditional probability equations in this study was an expanded version of the one used in D04. It was composed of 40-km grid-spacing RUC analysis soundings in 2001 and early 2002, and 20-km grid spacing analysis profiles that became operational thereafter through 2004. As in T03, these profiles consisted of 25-mb vertical level data and were associated with both tornadic and nontornadic supercell storms.

Supercells were determined both from radar (similar to T03) and also text indication of radar-detected storm rotation from National Weather Service (NWS) warnings (i.e., a radar-identifiable mesocyclone indicating a supercell). The majority of events were associated with tornado warnings (87%) and supercells that were clearly discrete (65%) from radar examination (i.e., not embedded within linear or other convective structures); however, only one-fourth (27%) of the cases verified with actual reported tornadoes. Therefore, the database provides an opportunity to examine environments for an abundance of supercell cases that were nontornadic, even though NWS personnel felt there was enough suggestion from radar and other sources to warrant tornado warnings for many of these storms.

All sounding profiles were valid within 110 km (roughly 70 statute miles) of the warned storm within the inflow region during the period 0–90 min prior to the initial warning time for the storm event. Additional information about this methodology is available from an earlier discussion of the database in D04. To better discriminate between weak or nontornadic supercells and those that produce significant [level 2 on the Fujita scale (F2)/EF2 or stronger] tornadoes, all profiles associated with F0/EF0 and F1/EF1 tornadoes were removed from this database. All profiles were situated within the eastern two-thirds of the United States (east of the Rocky Mountains) and spanned all 12 months of the year, with locations east of the plains well represented. The final database was composed of 557 RUC analysis soundings associated with supercells from 2001 through 2004. Significant tornadoes were associated with 153 soundings. Some additional information about the database is shown as part of Table 1.

Thermodynamic parameters of CAPE and CIN were computed using lowest 100-hPa mixed layer lifted parcels (denoted by the prefix ''ML''), as suggested by Craven et al. (2002). An important issue was instances (not uncommon) where RUC model output on analysis soundings proved to be too cool and/or dry in the lowest layer compared to surface observations at or very near the same location. Indeed, results from the RUC sounding database in T03 indicated that the largest model errors regarding moisture and temperature tended to be in the lowest portion of profiles near the ground. At SPC, the T03 results provided additional support for the hourly objective analysis scheme in the SPC mesoanalysis (Bothwell et al. 2002) that incorporates observed surface observations to at least partially correct for RUC errors at and near the surface. In the developmental database for this study, when similar errors occurred (defined as a difference of more than 1°F between the raw RUC surface data and the observed surface temperature and/or dewpoint at the same or closest surface observing site in the warm sector), actual temperature and dewpoint observations were utilized to modify the lowest levels of soundings by incorporating an objective algorithm when computing thermodynamic variables. This was done to obtain parameter values that were more representative of the true environments, similar to and consistent with the objective corrections employed by SPC to generate their hourly mesoanalysis used by forecasters around the country.

TABLE 1. Statistical summary of selected details and mean parameter values from the 2001–04 RUC developmental database across three seasonal groupings, by soundings associated with supercells producing significant tornadoes (SIGTOR; EF2 + intensity) and soundings associated with nontornadic supercells (SVR).

Description		Cool season 15 Oct–14 Apr	Spring 15 Apr–14 Jun	Summer/fall 15 Jun–14 Oct
Sounding totals	SIGTOR	48	65	40
	SVR	104	122	178
Discrete cells (%)	SIGTOR	52	86	75
	SVR	74	95	94
Tornado warned (%)	SIGTOR	100	98	98
	SVR	78	84	86
During diurnal max (2100–0300 UTC, in %)	SIGTOR	38	88	78
	SVR	62	70	78
During nighttime (0400–1200 UTC, in %)	SIGTOR	31	6	0
	SVR	20	18	8
Mean MLCAPE (J kg^{-1})	SIGTOR	1435	2628	3004
	SVR	898	1752	2056
Mean 0–6-km BWD (shr6; m s^{-1})	SIGTOR	30	27	23
	SVR	26	23	20
Mean 0–1-km SRH (m^2 s^{-2})	SIGTOR	288	232	136
	SVR	186	154	108
Mean 0–1-km BWD (shr1; m s^{-1})	SIGTOR	17	13	10
	SVR	13	10	8
Mean MLCIN (J kg^{-1})	SIGTOR	−23	−38	−20
	SVR	−57	−94	−60
Mean MLLCL (m)	SIGTOR	785	1111	1116
	SVR	955	1330	1370

4. Development of logistical regression equations

The description of a variety of convective parameters along with their individual statistics in RB98, T03, R03, D04, and T07 provided the background for the selection of all variables utilized in this research project. Following a period of experimentation with an assortment of these parameters (e.g., VGP, EHI, level of free convection, etc.), we decided to restrict our consideration of independent variables mainly to the basic components of the original version of STP [e.g., CAPE, 0–6-km bulk wind difference, 0–1-km SRH, and the lifted condensation level (MLLCL); see T03]. This was done because these components (and combinations thereof) are widely accepted in both research and operations as important assessment tools in tornado forecasting, and they provide a useful ''baseline'' comparison to STP for determining the operational utility of conditional probabilities. Our main research objectives were to 1) develop a set of statistically stable regression equations that were operationally useful and 2) design these equations in a way that would make physical sense to the meteorologists who would be using them.

Mean seasonal values of component parameters from our 2001–04 RUC developmental database described in the previous section are shown in Table 1 for significant supercell tornadoes (SIGTOR) versus nontornadic supercells (SVR).

Note that where ''shr'' is part of a parameter/variable name indicating a straight-line vector shear magnitude, we utilize the bulk wind difference (BWD) in all instances (i.e., shr6 is the bulk wind difference between the surface and 6 km AGL, and shr1 is the computed bulk wind difference in the lowest kilometer of the atmosphere). For the purpose of displaying discrimination attributes for selected independent variables, we followed the approach of Brooks and Craven (2002) and plotted cumulative distribution functions (CDFs) for both significant tornadic and nontornadic supercell populations.

It was decided to combine two components from the original version of STP, buoyancy and 0–6-km bulk wind difference, similar to the ''CAPE × 0-6 km shear'' parameter developed by Brooks and Craven (2002). This is because combinations of CAPE and deep-layer shear are related to dynamic stretching through parcel buoyancy and lift via vertical pressure gradients generated by updraft interaction with vertical shear, and are key assessment parameters for determining supercell potential, an important prerequisite for assessing supercell tornado potential. To provide a more responsive signal across a broad range of CAPE–shear combinations, this variable was computed as the product of the square root of CAPE (J kg^{-1}) with the 0–6-km bulk wind difference (shr6, m s^{-1}), reflecting basic parcel theory where peak updraft strength W_{max} is related to the square root of

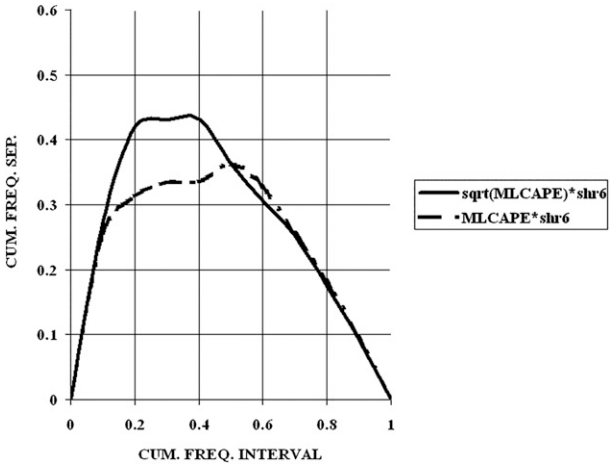

FIG. 1. Separation in cumulative frequencies between significant supercell tornadoes and nontornadic supercell populations as a function of (MLCAPE × shr6) for the RUC database during 2001–04 as described in the text.

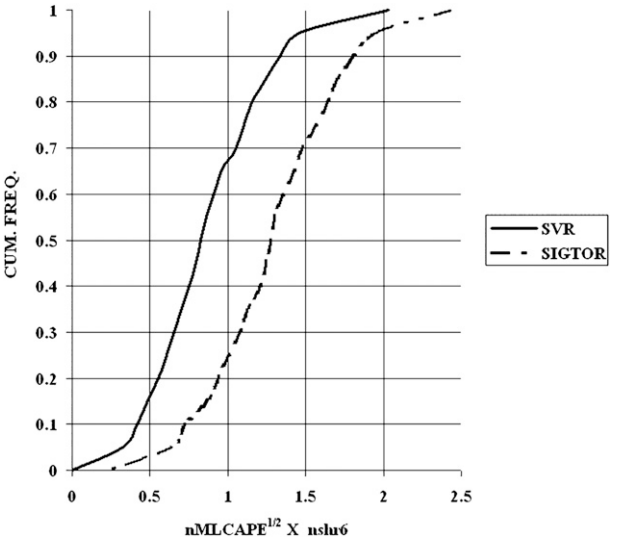

FIG. 2. CDFs for the product of the normalized square root of MLCAPE (J kg^{-1}) and the normalized 0–6-km bulk wind difference (shr6; m s^{-1}), for the RUC database during 2001–04 as described in the text. Significant supercell tornadoes (SIGTOR; EF2+) are shown by dashed black lines and nontornadic supercells (SVR) are shown by solid black lines.

CAPE, ignoring effects such as mixing and water loading. Figure 1 shows the differences in cumulative frequency separation between significant tornadic and nontornadic supercell storms in the development database when comparing the use of the square root of MLCAPE to the use of MLCAPE directly. Figure 1 confirms that incorporation of the square root provides better separation between the two groupings, and is particularly evident between cumulative frequencies from roughly 0.2 to 0.4. The CDF plot for the product of the square root of CAPE and the 0–6-km bulk wind difference is shown in Fig. 2, comparing significant tornadoes (SIGTOR) to nontornadic supercells (SVR).

The CDF plot for a third component, 0–1-km SRH (hereafter SRH, m^2 s^{-2}), is displayed in Fig. 3. The SRH parameter is a measure of horizontal streamwise vorticity available for vertical tilting into a storm updraft to induce low-level rotation (e.g., Davies-Jones et al. 1990; Wicker 1996), and scored well as a discriminator in R03 (as did 0–1-km EHI). It is widely recognized and used operationally as an important ingredient contributing to tornadic supercell environments.

The final component from the original version of STP, MLLCL (m), is shown in the CDF plot in Fig. 4. Both RB98 and R03 discuss the physical role that low MLLCL heights may play with respect to tornado development through the diminishment of evaporation beneath precipitating storm bases and the resulting reduction of cold-air outflow. The work of Brooks and Craven (2002) also indicated a relationship between 0- and 1-km bulk wind shear and MLLCL height regarding tornado frequencies, suggesting the possible utility of combining these components, explored later in this section.

An additional component also considered was MLCIN (J kg^{-1}). Results from D04 and T07 indicate that the degree of MLCIN is in many cases an important thermodynamic discriminator between tornadic and nontornadic supercell populations. Smaller MLCIN suggests

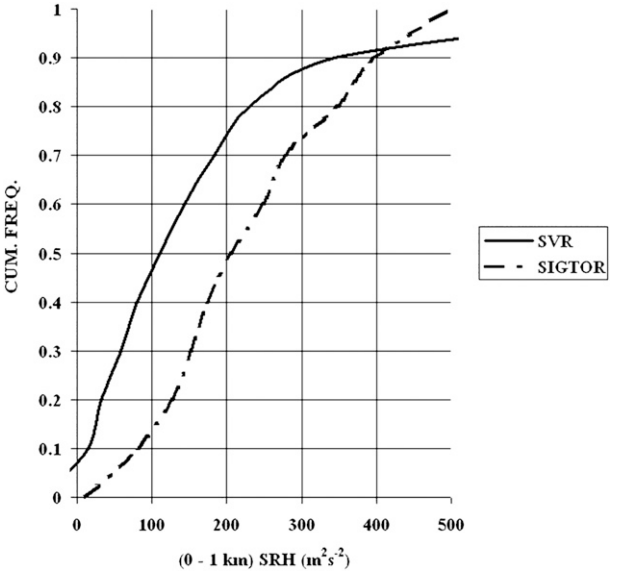

FIG. 3. As in Fig. 2, but for 0–1-km SRH (m^2 s^{-2}) as described in the text.

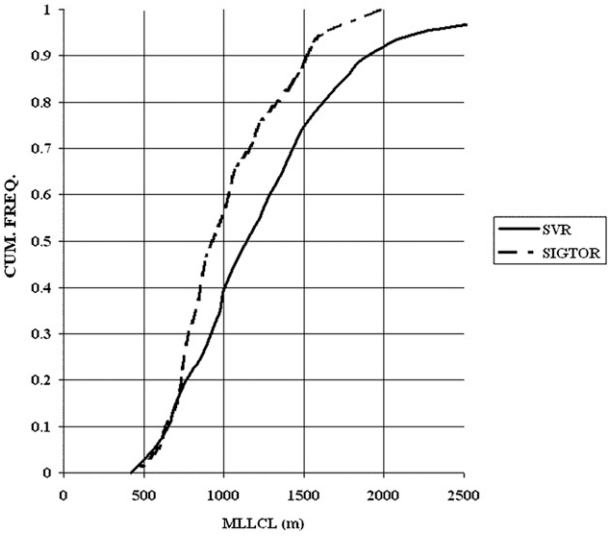

FIG. 4. As in Fig. 2, but for MLLCL (m) as described in the text.

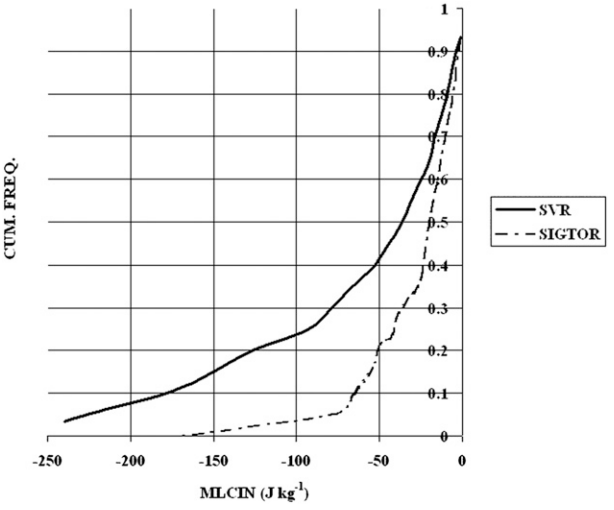

FIG. 5. As in Fig. 2, but for MLCIN (J kg^{-1}) as described in the text.

a relatively surface-based environment, while larger MLCIN can inhibit the tilting and stretching of low-level SRH and shear. This parameter was added to a later version of STP (Thompson et al. 2011). The CDF plots for this additional component are displayed in Fig. 5.

A final component considered was 0–1-km bulk wind difference (shr1, m s^{-1}), mainly as a potential substitute for SRH, and noted earlier in conjunction with MLLCL from Brooks and Craven (2002). This was included because shr1 does not require a storm-motion estimate, and is not dependent on the specification of the detailed low-level hodograph structure. Brooks and Craven (2002) found that tornadic environments tend to be characterized by larger values of shr1. Furthermore, the bulk wind difference in the 0–1-km AGL layer shows a significant correlation to SRH, as can be seen in the scatterplot of SRH versus shr1 shown in Fig. 6 for all supercells in our development database.

Logistic regression results for this research were obtained online through the Interactive Statistical Calculation Pages (http://statpages.org/logistic.html). Several logistical regression equations generating conditional probabilities for significant tornadoes were developed and tested. All were composed of three terms of variables (some terms as combinations of two variables, and other terms as stand-alone variables) through experimenting with the original STP components and additional components as discussed above. The equations tested generally took the following form to relate to supercell tornado ingredients and processes: 1) the first term of variables (or first independent variable) related to supercell potential through combining MLCAPE and shr6 as discussed earlier; 2) the second term of variables (or second independent variable) related more specifically to tornado potential via low-level shear in the form of SRH or shr1, sometimes combined with MLLCL (see Brooks and Craven 2002); and 3) the third term (or third independent variable) used MLCIN as a stand-alone variable and limiting factor.

After several different equations were tested, we were able to obtain three equations that were statistically significant as logistic regression relationships. These are presented here in descending order of their chi square scores. The first logistic regression equation took the form

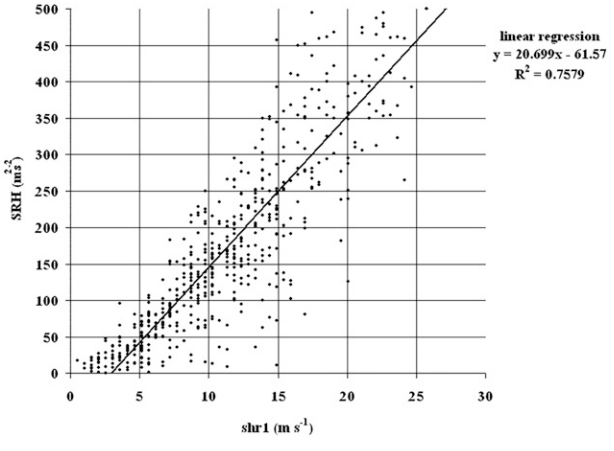

FIG. 6. Scatter diagram with least squares regression line for 0–1-km SRH (m^2 s^{-2}) as a function of 0–1-km bulk wind difference (shr1, m s^{-1}) from the RUC database during 2001–04 as described in the text.

TABLE 2. Statistical summary for logistic regression Eq. (1). Independent variables 1–3 in Eq. (1) are 1) the product of the normalized square root of MLCAPE (J kg^{-1}) and the normalized 0–6-km bulk wind difference (shr6, m s^{-1}), 2) the normalized 0–1-km SRH (m^2 s^{-2}), and 3) the normalized MLCIN (J kg^{-1}) as described in the text.

Overall model fit			
Chi square = 256.5138, df = 3, p = 0.0000			
Variable	Coef	Std error	P
1	2.9814	0.3659	0.0000
2	1.6658	0.1957	0.0000
3	1.8234	0.2541	0.0000
Intercept = −4.6886			
Odds ratios (OR) and 95% confidence interval			
Variable	OR	Low	High
1	19.7160	9.6234	40.3926
2	5.2899	3.6049	7.7624
3	6.1930	3.7635	10.1911

$$-4.69 + 2.98[n(\sqrt{\text{MLCAPE}})n(\text{shr6})] + 1.67n(\text{SRH}) + 1.82n(\text{MLCIN}), \quad (1)$$

which is the $f(x)$ portion of the logistic regression equation in its generalized form:

$$P = \frac{1}{\{1 + \exp[-f(x)]\}}. \quad (1a)$$

This particular equation uses SRH instead of shr1; also notice that MLLCL is not utilized, which will be discussed shortly. Because logistic regression is a binary form of regression, the P in relation (1a) above equates to the probability of the occurrence of 1 [i.e., $P(Y = 1)$], which is synonymous with significant tornado occurrence. Thus, all nontornado reports are coded with $Y = 0$ while significant tornado reports are coded as $Y = 1$.

The $n(\cdot)$ notation in Eq. (1) denotes that a component is normalized to the developmental database sample mean for that component. This was done to provide similar weighting for each term in the equation; otherwise, the magnitude of the first term (MLCAPE and shr6 combined) would often dominate the equation results. We normalized each of the components in Eq. (1) as follows: 40.7 J kg^{-1} for the square root of MLCAPE, 23.4 m s^{-1} for shr6, 164.8 m^2 s^{-2} for SRH, and 58.1 J kg^{-1} for MLCIN. Note that MLCIN values input into this equation are negative numbers (indicating negative buoyancy), but the normalizing factor is a positive number resulting in a decrease of the equation sum and conditional probability for tornadoes as absolute values of MLCIN increase. A statistical summary for Eq. (1) is provided in Table 2.

TABLE 3. As in Table 2, but for logistic regression Eq. (2). The normalized 0–1-km bulk wind difference (shr1, m s^{-1}) is used as the second independent variable.

Overall model fit			
Chi square = 243.6602, df = 3, p = 0.0000			
Variable	Coef	Std error	P
1	3.1108	0.3633	0.0000
2	2.2267	0.2758	0.0000
3	1.3799	0.2113	0.0000
Intercept = −5.6731			
Odds ratio and 95% confidence interval			
Variable	OR	Low	High
1	22.4384	11.0081	45.7374
2	9.2694	5.3985	15.9160
3	3.9744	2.6269	6.0131

When shr1 is substituted for SRH as the second term, the following logistic regression equation results:

$$-5.67 + 3.11[n(\sqrt{\text{MLCAPE}})n(\text{shr6})] + 2.23n(\text{shr1}) + 1.38n(\text{MLCIN}). \quad (2)$$

In Eq. (2), a normalization coefficient of 11 m s^{-1} is used for shr1. Table 3 provides a statistical summary for this equation.

Finally, a third equation includes MLLCL in the second term as a variable in combination with shr1 (after Brooks and Craven 2002):

$$-4.73 + 3.21[n(\sqrt{\text{MLCAPE}})n(\text{shr6})] + 0.78[n(\text{shr1})/n(\text{MLLCL})] + 1.06n(\text{MLCIN}). \quad (3)$$

Table 4 provides a statistical summary for Eq. (3), and a normalization coefficient of 1170 m is used for MLLCL.

Surprisingly, Eq. (3) had the poorest chi square score of the three statistically significant equations shown here. It is difficult to account for why Eqs. (1) and (2) without MLLCL scored better than Eq. (3) with MLLCL, except to note that the CDF plot for MLLCL in Fig. 4 visually showed less separation between SIGTOR and SVR (nontornadic supercell) events across a typical range of operational values than with CDF plots for any of the other components. This could suggest that, outside of very high MLLCL heights (e.g., near and above 2000 m), MLLCL contributes less information (on average) toward discriminating between tornadic and nontornadic environments than the other components.

TABLE 4. As in Table 2, but for the logistic regression in Eq. (3). The normalized 0–1-km bulk wind difference (shr1, m s^{-1}) divided by the normalized MLLCL (m) is used as the second independent variable.

Overall model fit			
Chi square = 214.6549, df = 3, p = 0.0000			
Variable	Coef	Std error	P
1	3.2111	0.3507	0.0000
2	0.7800	0.1139	0.0000
3	1.0559	0.1923	0.0000
Intercept = −4.7285			
Odds ratios and 95% confidence interval			
Variable	OR	Low	High
1	24.8075	12.4761	49.3274
2	2.1815	1.7451	2.7272
3	2.8745	1.9718	4.1907

This is not to say that MLLCL is unimportant in individual cases. However, in a ''bulk'' sense, all attempts made to utilize MLLCL, as a stand-alone variable, resulted in high p scores that suggested an unstable/unreliable regression relationship.

In this paper, because of the better chi square scores for Eqs. (1) and (2) (see Tables 2 and 3) and limited space, we have elected to present results only from those two equations due to their relative simplicity and improved scoring. For simplicity hereafter, the two regression equations from this section will be referred to, respectively, as EQU(SRH) and EQU(shr1).

5. Statistical evaluation of regression equations from 2008 storm data

a. Independent verification database

To perform an independent statistical evaluation for EQU(SRH) and EQU(shr1), severe weather reports associated with both supercells and nonsupercells for 2008 was tallied over 40 km × 40 km gridded fields by SPC staff. From this, an hourly verification database was developed that included 1) the total of separate storm reports for each grid, 2) a separate flag for significant and nonsignificant tornadoes, 3) a designator as to whether a supercell was identified within the grid, 4) a delineator as to whether the supercell was discrete or nondiscrete, 5) computed probability values from EQU(SRH) and EQU(shr1) along with effective STP values, and 6) interpolated values for the components/variables utilized in the logistic regression formulas. More information on the preparation of this type of database can be found in Schneider and Dean (2008).

For our purposes, the only portion of the database utilized for verification was that flagged for the presence of supercells. This file contained data for 1695 supercells, 1031 of which were nondiscrete and 664 of which were discrete. Although not an exhaustive listing of supercells that occurred during 2008, the verification database generally matched operational conditions of the original 2001–04 developmental database because the data were associated with identified supercells when local NWS offices would likely be issuing a variety of severe weather warnings during the same time frame. The composition of discrete versus nondiscrete supercells for our verification database contrasted with the developmental database (where a majority of supercells were discrete storms), but the 2008 supercell sample was still quite useful for testing our regression equations because of its large size.

Significant tornado frequency was 12.7% for the discrete sample in the verification database, and 10.3% for the nondiscrete supercells. A total of 50 supercell cases in the 2008 database were likely elevated supercells with MLCAPE values of zero. In these cases, although a nonzero equation value could be obtained by evaluating the other nonzero equation terms, it was decided that these probability values would not be physically meaningful without MLCAPE present for evaluating updraft potential. Therefore, in the verification exercise, similar to the database in T03, conditional probabilities for both equations were set to zero for these elevated cases.

b. Statistical verification

One means of accomplishing a statistical verification for any new forecast technique is to provide comparative statistics between the new technique and an accepted standard. The most recent version of STP (effective-layer STP; Thompson et al. 2011) provides such a standard because it is used operationally as severe thunderstorm and tornado forecast guidance by NWS forecasters.

Because the regression equations output a conditional probability value, while STP consists of a dimensionless value, direct comparison between the two is not exactly straightforward. However, computation of relative operating characteristic curves (ROCs; Mason 1982; Stanski et al. 1989) from signal detection theory provides one useful means of comparing relative skill. In Fig. 7a, the ROC curves for EQU(SRH) and effective-layer STP are displayed; Fig. 7b provides comparative ROC curves for EQU(shr1) and effective-layer STP. A ROC diagram indicates forecast skill by the positive area between an individual ROC curve and the diagonal line representing a no-skill forecast that incurs false alarms at the same rate as hits (i.e., net positive skill is indicated where the ROC curve data points are plotted above the diagonal line).

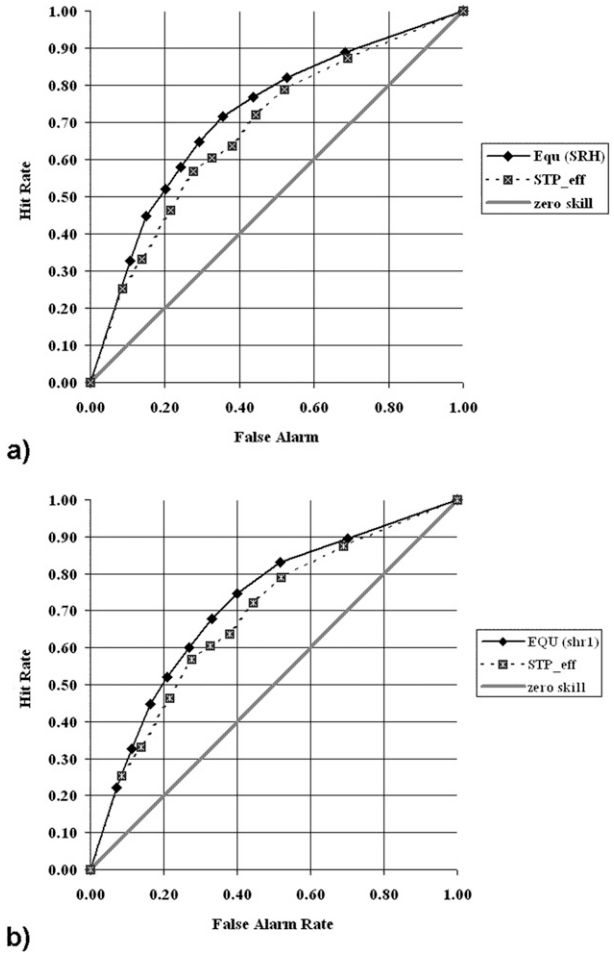

FIG. 7. (a) ROC curves for logistic regression EQU(SRH) (solid black) and effective-layer STP (dashed black) from the 2008 verification database of 1695 supercells as described in the text. (b) As in (a), but for EQU(shr1).

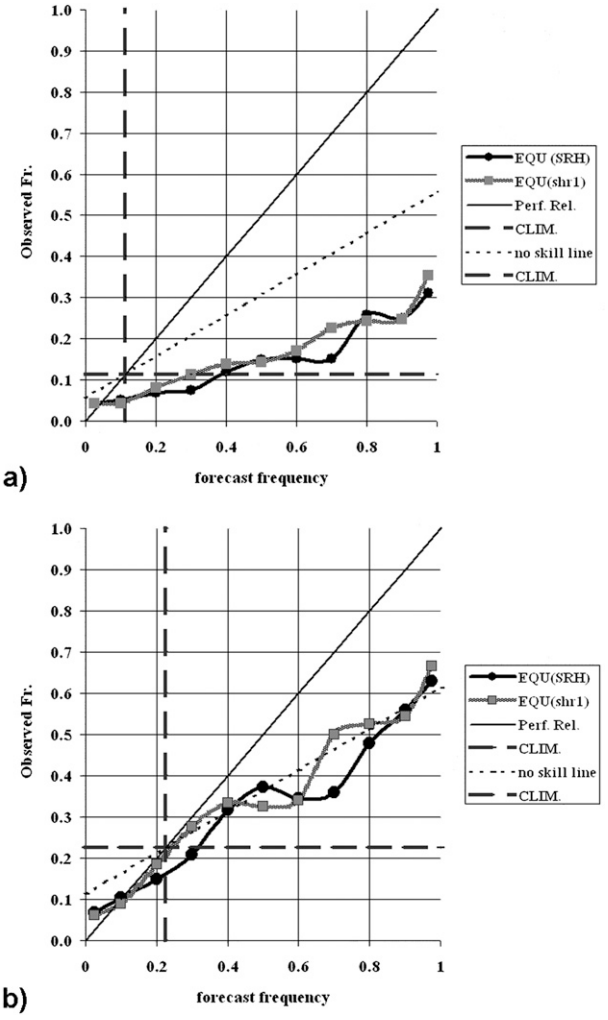

FIG. 8. (a) Attributes diagram for EQU(SRH) (black chain) and EQU(shr1) (gray chain) from the 2008 verification database of 1695 supercells as described in the text. The lines for perfect reliability and for no skill are indicated by solid and short-dashed lines, respectively. Climatology (vertical and horizontal) is shown in thick long dashed lines. (b) As in (a), but for cases with weak (i.e., EF0 and EF1) tornadoes removed from the database, leaving a total of 846 supercells.

We employed numerical integration to compute the area under the ROC curves for the regression equations and effective-layer STP in Figs. 7a and 7b using Simpson's approximation. The areas under the individual ROC curves in Figs. 7a and 7b are 0.720, 0.718, and 0.684 for EQU(SRH), EQU(shr1), and STP, respectively. Thus, EQU(SRH) results show modest improvement (5.3%) over effective-layer STP, and the EQU(shr1) results indicate slightly less improvement (5.0%).

It should be noted that, with close examination of each ROC curve, both regression equations display the relative improvement over the effective-layer STP beginning in the lower probability ranges (i.e., 20%–35%), and that relative skill maximizes in the middle probability ranges. This improved performance in the lower probability range may have positive implications for anticipating areas of developing tornado threats with potential for improved lead times in some tornado cases.

To further examine the statistical verification and potential forecast skill of our regression equations, attributes diagrams (Wilks 2006) were constructed using two different versions of the 2008 supercell verification database in Figs. 8a and 8b. The heavy dashed vertical and horizontal lines in these attributes diagrams represent climatological frequencies, while the angled dotted line represents no skill (the line halfway between the solid perfect reliability line and the horizontal

TABLE 5. Conditional probability verification for EQU(SRH) and EQU(shr1) as a function of cell mode for the 2008 supercell verification database; data include SIGTOR percentage for supercell totals broken down across probability intervals of 20%. See text for additional details.

Conditional probability EQU(SRH) (discrete supercells)	SIGTOR (%)	SIGTOR cases	Supercell totals
80%–100%	34.5	40	116
60%–<80%	24.3	17	70
40%–<60%	10.2	6	59
20%–<40%	9.0	9	100
0%–<20%	3.8	12	319
Totals		84	664
Conditional probability EQU(SRH) (nondiscrete supercells)	**SIGTOR (%)**	**SIGTOR cases**	**Supercell totals**
80%–100%	22.1	34	154
60%–<80%	15.6	15	96
40%–<60%	12.3	15	122
20%–<40%	9.8	16	164
0%–<20%	5.3	26	495
Totals		106	1031
Conditional probability EQU(shr1) (discrete supercells)	**SIGTOR (%)**	**SIGTOR cases**	**Supercell totals**
80%–100%	34.9	30	86
60%–<80%	28.0	21	75
40%–<60%	15.7	11	70
20%–<40%	9.5	9	95
0%–<20%	3.8	13	338
Totals		84	664
Conditional probability EQU(shr1) (nondiscrete supercells)	**SIGTOR (%)**	**SIGTOR cases**	**Supercell totals**
80%–100%	24.1	26	108
60%–<80%	17.1	18	105
40%–<60%	10.9	14	129
20%–<40%	11.8	19	161
0%–<20%	5.5	29	528
Totals		106	1031

climatological frequency line). To show positive forecast skill, points on the right side of the vertical climatological frequency line must be above the no-skill line, and on the left side must be below the no-skill line. Notice in Fig. 8a (the full unfiltered database) that negative forecast skill is indicated for both equations on the right side of the diagram, but positive skill is indicated on the far left side. This suggests that the skill of both EQU(SRH) and EQU(shr1) is in lower-probability tornado forecasts, as noted with the ROC curves earlier.

Moreover, the negative forecast skill of EQU(SRH) or EQU(shr1) on the right side of Fig. 8a is considerably reduced when the 2008 verification database is pared down by removing weaker tornado reports (EF0 and EF1) from the database (see Fig. 8b, showing a subset composed of SIGTOR events and nontornado events). Notice that the skill lines for both equations on the right side of Fig. 8b are much closer to the no-skill line, with even some occasional positive skill indicated. This suggests that when isolated weak supercell tornadoes associated with localized and often difficult-to-detect environmental factors are removed from the database (a situation where the equations would not be expected to perform well), the equations may perform somewhat better across a broader spectrum of tornado frequency situations, while retaining the notable lower-probability tornado forecast skill discussed earlier.

Probability performance values for both EQU(SRH) and EQU(shr1) are presented in Table 5, breaking the metrics into separate groupings for discrete supercells and nondiscrete supercells. Although the general trend toward higher tornado frequencies with higher probabilities is quite evident, it is also seen that both regression equations do a better job partitioning risk for the discrete supercell sample compared to the nondiscrete sample. This suggests that the regression equations and resulting probabilities will verify best in operational settings where discrete supercells occur, an important issue for forecasters to keep in mind.

The following section examines conditional probability graphics generated from 2008 through some brief tornado case examinations.

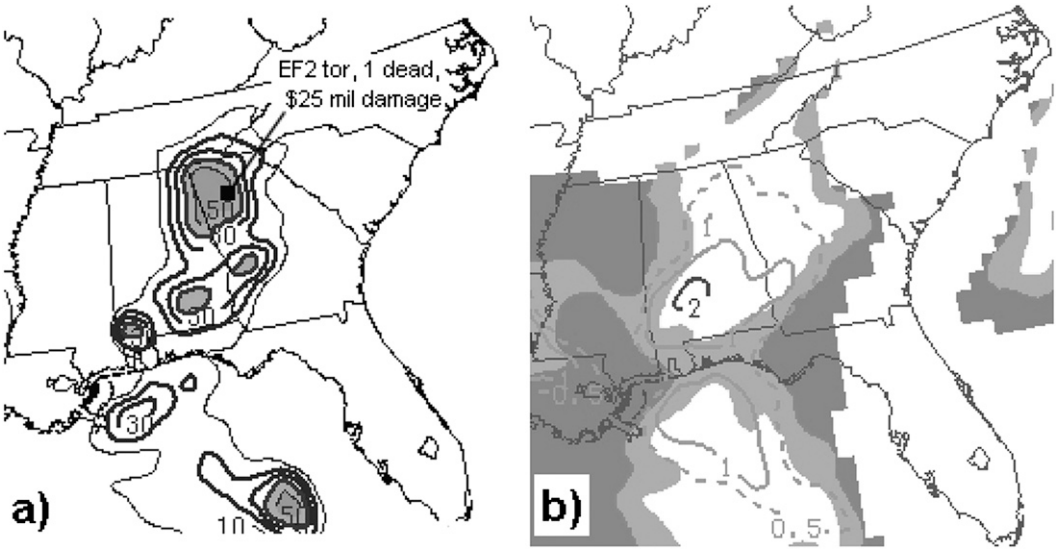

FIG. 9. Graphics from SPC mesoanalysis at 0100 UTC 15 Mar 2008, showing (a) conditional probabilities from EQU(SRH) and (b) effective-layer STP over the southeastern United States, both utilizing the lowest 100-hPa mixed-layer lifted parcels. In (a), conditional probabilities are contoured and labeled at 10% intervals, with values ≥40% shaded. In (b), STP values (dimensionless) are contoured at 0.5 (shaded dashed line), 1.0 (shaded solid line), and 2.0 (dark solid line), with light shading for MLCIN values −25 to −99 J kg^{-1}, and dark shading for MLCIN −100 J kg^{-1} and less. In (a), the location of an EF2 tornado at 0140 UTC is shown (square dot) and labeled.

6. Operational test and evaluation of the conditional probability output and performance during three 2008 events

a. SPC–NWS collaboration

Graphical output from the SPC hourly mesoanalysis system (Bothwell et al. 2002) has been provided to staff at the NWS Chanhassen, Minnesota, Weather Forecast Office (WFO MPX) for operational testing and evaluation of the regression equations. The displays are typically available 30–40 min past each hour; all graphics are archived at SPC for purpose of review and/or case studies. In addition, prognostic output fields from the regression equations in this study using gridded data from operational numerical weather prediction models are available in the local WFO Advanced Weather Interactive Processing System (AWIPS) for use by MPX forecasters.

The forecast staff has provided favorable feedback on the conditional probability graphics. However, it is emphasized that an awareness of individual component values and fields, along with the evolving surface patterns and convective mode, must be maintained to determine if conditional probability values and fields make physical sense. For example, in situations with strong warm/moist advection, it is possible that sizable MLCIN along and north of a warm front can dominate and reduce conditional tornado probability values in an environment also characterized by large values of SRH and deep-layer shear (e.g., see the final case in section 6b). Forecasters aware of the evolving surface pattern and potential for eroding CIN will know to adjust tornado probability values upward along warm frontal zones and areas of rapid warm advection. In addition, recognition of the ongoing convective mode always needs to be incorporated into warning decisions. An overforecast bias of tornado probabilities will be especially evident when observed convection is linear or transitioning toward that mode. It is imperative that forecasters not use the probability output as an isolated "shortcut" or stand-alone product. More information about the proper use and interpretation of indices and composite parameters is found in Doswell and Schultz (2006).

b. Case examples from 2008

In section 5b, it was seen from the ROC curves that conditional probability output from both regression equations generally performed as well or occasionally slightly better than the effective-layer STP. A case where conditional probabilities from both regression equations devised in this study provided better guidance than STP occurred on 14 March 2008. An evening supercell near a surface stationary front (not shown) produced an EF2 intensity tornado that struck downtown Atlanta, Georgia, around 0140 UTC 15 March

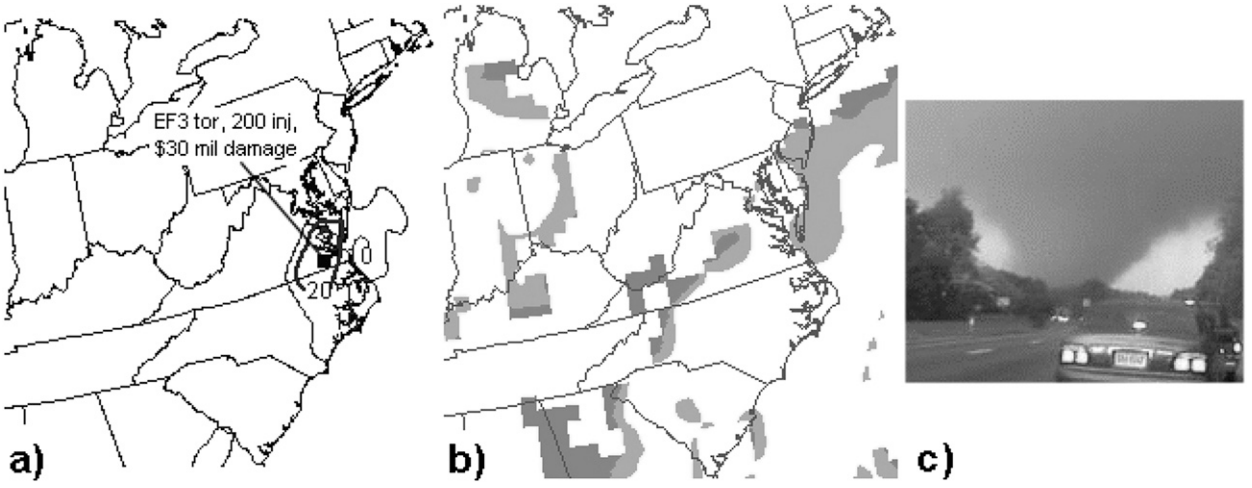

FIG. 10. As in Fig. 9, but at 1900 UTC 28 Apr 2008 over the central Atlantic coast region. In (a), the location of an EF3 tornado at 2005 UTC is shown (square dot) and labeled. [The photo of the Suffolk, VA, EF3 tornado in (c) is courtesy of Marsha Mears and WAVY-TV.]

2008, killing one person. Graphical output for EQU(SRH) and effective-layer STP at 0100 UTC is shown in Fig. 9. The conditional probability field derived using EQU(SRH) in Fig. 9a focused a higher threat for significant supercell tornadoes (>50%) over northern Georgia that evening. In contrast, the estimated field for effective-layer STP (Fig. 9b) suggested that the supercell tornado potential was more favored farther south and southwest.

A second case illustrating the potential benefits of the regression equations occurred on 28 April 2008 when a supercell producing an EF3 tornado struck Suffolk, Virginia, around 2005 UTC. Graphical output results from the SPC mesoanalysis for EQU(SRH) and effective-layer STP at 1900 UTC are shown in Fig. 10. This tornado injured 200 people and was the strongest of a cluster of tornadoes that occurred over southeast Virginia that afternoon to the south of a surface warm front (not shown). Notice that EQU(SRH) (Fig. 10a) suggested at least a low-end conditional probability (>20%) of significant tornadoes this day, while significant tornado potential appeared to be minimal based on STP values (Fig. 10b) of less than 0.5.

A third case is shown in Fig. 11 over northeastern Colorado on 22 May 2008, when a supercell producing an unusual late-morning EF3 tornado struck the town of Windsor just before 1800 UTC, killing one person and causing nearly $150 million in damage. Graphical output from the SPC mesoanalysis at 1700 UTC is shown in Fig. 11. As in the 15 March 2008 case, EQU(SRH) (Fig. 11a) suggested higher probabilities (>50%) in a localized area over northeastern Colorado, with probabilities as high as 62% for EQU(SRH) and 65% for EQU(shr1) (not shown). Although the effective-layer STP (Fig. 11b) did show a small area of values that exceeded 1.0 over northeastern Colorado, EQU(SRH) appeared to be more useful in graphically highlighting significant tornado risk with developing storms along a stationary front (not shown) north of Denver. An hour later, the STP pattern (Fig. 11d) showed no substantial change, but the EQU(SRH) graphic (Fig. 11e) highlighted increasing risk along the Colorado–Wyoming border, where an EF2 tornado at 1910 UTC developed with the same supercell and tracked northwest for 25 mi, causing damage in Laramie, Wyoming.

It is also worth noting that during the late afternoon on the same day as in Fig. 11 (22 May 2008), a localized outbreak of several tornadoes took place over northwest Kansas. Notice that already by early afternoon both EQU(SRH) and STP in Figs. 11a, 11b, 11d, and 11e were highlighting the environment in northwest Kansas near a surface warm front (not shown) where tornadoes began occurring a few hours later. From recent forecaster experience, this is representative of how both equations developed in this study and STP tend to handle more ''typical'' supercell tornado environments and events.

As would be expected, there are instances where the effective-layer STP will outperform both regression equations, given the nearly equal ROC scores indicated from the 2008 verification data. An example of superior STP performance occurred on 2 May 2008 in northeast Mississippi when an EF2 tornado developed around 2245 UTC from a supercell in Union County, Mississippi, causing $250,000 in damage. Effective-layer STP values from the SPC mesoanalysis were close to 2.0 over northeast Mississippi at 2200 UTC (Fig. 12b), but EQU(SRH) (Fig. 12a) did not show a risk in the same

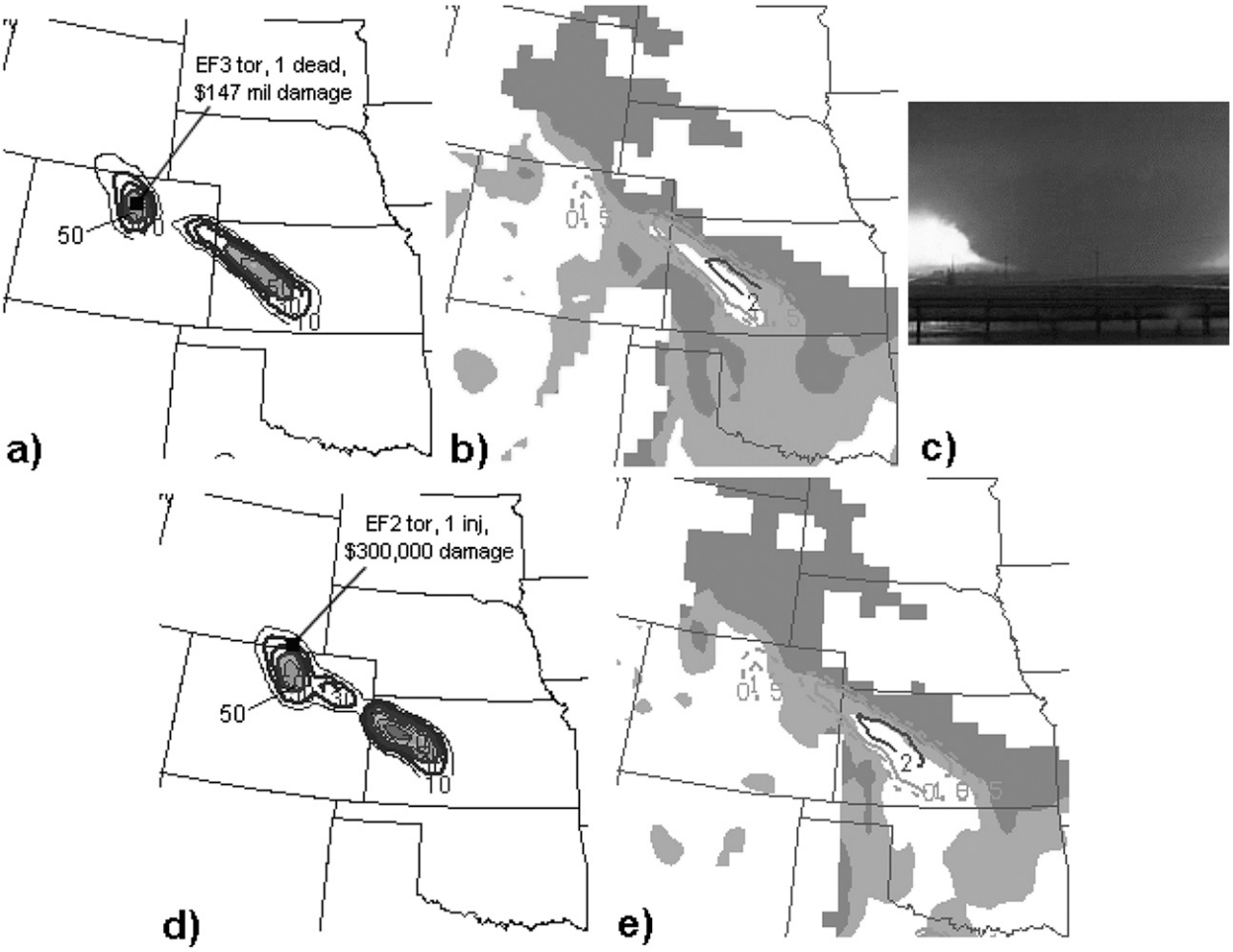

FIG. 11. As in Fig. 9, but at (a),(b) 1700 and (d),(e) 1800 UTC 22 May 2008 over the central high plains region. (c) Video image of the Windsor, CO, EF3 tornado (courtesy of KUSA-TV). In a), location of this tornado at 1730 UTC is shown (square dot) and labeled. In (d), the location of an EF2 tornado at 1910 UTC is shown (square dot) and labeled.

specific area. In this case, MLCIN values near −100 J kg^{-1} on the eastern fringe of strong warm/moist advection appeared to dominate the solution for both equations in spite of large SRH and shr1 values (around 300 m^2 s^{-2} and 32 kt, or 16.5 m s^{-1}, respectively; not shown). Radar imagery (not shown) also indicated several discrete, surface-based cells approaching Union County in the 30 min prior to the EF2 tornado, and an examination of both radar and individual equation components, along with STP, would likely have alerted forecasters to the increased tornado risk over northeast Mississippi.

In addition to using composite output from sources such as EQU(SRH) and EQU(shr1) developed in this study, the example cases above underscore forecaster responsibility to 1) always examine individual environmental background parameters carefully and 2) combine this information with radar evidence to formulate the best possible warning decision.

7. Summary and concluding discussion

Two physically based logistic regression equations that estimate the conditional probabilities of significant tornadoes from environmental background parameters have been described in detail. Statistical verification with an independent dataset of 1695 supercells, organized and gathered by SPC staff, reveals that both equations generally perform as well or slightly better than SPC's effective-layer STP.

A limitation in utilizing either of the regression equations is that significant tornado risk is overestimated over all brackets of probability with the exception of the lowest bracket. The main reason for the problem of probability overestimation is due to the fact that the predictands for these equations are an occurrence of a rare event (see Brooks, 2004). Nevertheless, the equation output is still very useful in that it captures the tendency for increasing

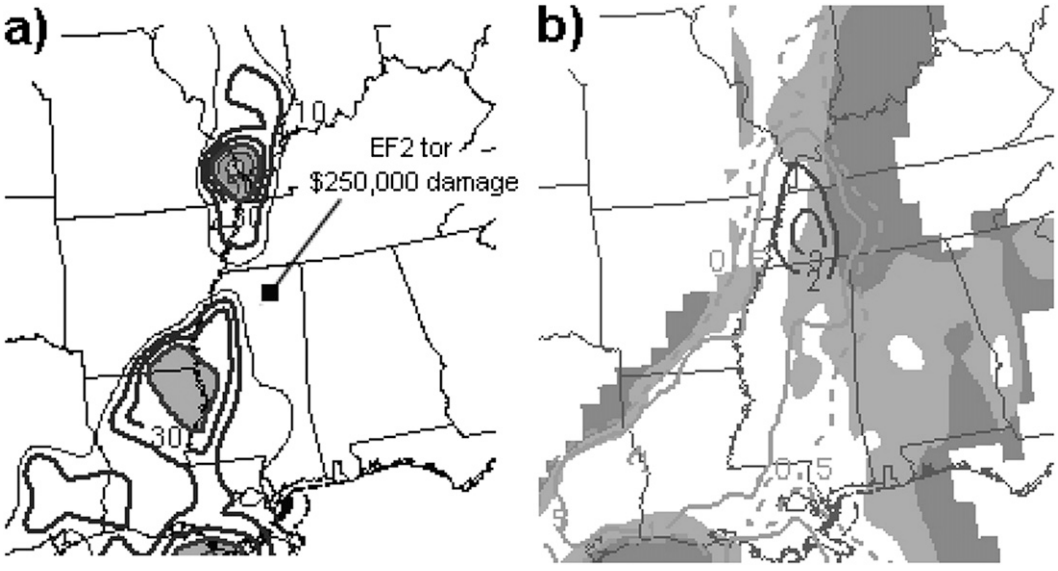

FIG. 12. As in Fig. 9, but at 2200 UTC 2 May 2008 over the lower Mississippi Valley region. In (a), the location of an EF2 tornado at 2245 UTC is shown (square dot) and labeled.

levels of tornado risk (including both significant and nonsignificant tornadoes and combinations of such storms) with increasing probability. As forecasters work with these equations and develop a learning curve with respect to their performance under various severe weather scenarios, there may be improvement in the false alarm warning metric as well as an earlier assessment of severe weather potential with some events that could help with staffing decisions. In addition, as monitored conditional probability rises or drops over time, the opportunity exists to communicate these changes directly to the public.

However, both equations (as well as effective STP) do have a tendency to overestimate significant tornado risk where the initial convective mode is nondiscrete, or where the mode evolves from discrete to linear. This is not unexpected, since explicit information about the convective mode is not incorporated into these formulations. In addition, it has also been noted from operational use that significant tornado events frequently occur along gradients of conditional probability, particularly to the north and west of probability maxima using either equation. This tendency has also been noted regarding effective-layer STP by SPC staff (S. Weiss 2009, personal communication) and by Cohen (2010).

Future research efforts might focus on determining the physical nature of this apparent tendency. For example, prior research has shown that many tornadoes occur along or near boundaries (Maddox et al. 1980; Markowski et al. 1998), such as warm fronts in areas of strong warm advection where wind shear, instability, and surface convergence are strongly focused. Because these boundaries are typically associated with probability gradients from our equations, this may help explain the association of tornadoes within many such gradients.

In conclusion, the regression equations developed in this research and effective-layer STP are seen as complementary to one another and will help support local warning decisions at NWS forecast offices. Accordingly, plans are under way to add the conditional probability of significant tornadoes to the SPC mesoanalysis Web page (http://www.spc.noaa.gov/exper/mesoanalysis/).

Acknowledgments. The authors thank Science and Operations Officers Steve Weiss of the SPC and Tom Hultquist of the Twin Cities Forecast Office for their thoughtful reviews of this work. It would have been impossible to realistically verify any of our work without the hours of labor of Richard Thompson and Bryan Smith at the SPC in assembling a suitable storm mode classification database for completing the 2008 supercell verification exercise. Richard Thompson and two anonymous reviewers also provided invaluable interpretation of our statistical work and helped us clarify a number of our key research findings. In addition, we thank Dr. Louis Uccellini for his continuous encouragement on this project from its inception. Computer software required for the statistical portion of this research was provided by Dr. John C. Pezzulo. Finally, the first author would like to dedicate this research to the late Professor Lyle Horn at the University of Wisconsin—Madison.

REFERENCES

Benjamin, S. G., and Coauthors, 2004: An hourly assimilation cycle: The RUC. *Mon. Wea. Rev.,* **132,** 495–518.

Bothwell, P. D., J. A. Hart, and R. L. Thompson, 2002: An integrated three-dimensional objective analysis scheme in use at the Storm Prediction Center. Preprints, *21st Conf. on Severe Local Storms,* San Antonio, TX, Amer. Meteor. Soc., J117–J120.

Brooks, H. E., 2004: Tornado warning performance in the past and future: A perspective from signal detection theory. *Bull. Amer. Meteor. Soc.,* **85,** 837–843.

——, and J. P. Craven, 2002: Database of proximity soundings for significant severe thunderstorms, 1957–1993. Preprints, *21st Conf. on Severe Local Storms,* San Antonio, TX, Amer. Meteor. Soc., 639–642.

——, C. A. Doswell III, and R. B. Wilhelmson, 1994: On the role of midtropospheric winds in the evolution and maintenance of low-level mesocyclones. *Mon. Wea. Rev.,* **122,** 126–136.

Cohen, A. H., 2010: Indices of violent tornado environments. *Electron. J. Oper. Meteor.,* EJ6. [Available online at http://www.nwas.org/ej/2010-EJ6/.]

Colby, F. P., 1984: Convective inhibition as a predictor of convection during AVE-SESAME II. *Mon. Wea. Rev.,* **112,** 2239–2252.

Craven, J. P., R. E. Jewell, and H. E. Brooks, 2002: Comparison between observed convective cloud-base heights and lifting condensation level for two different lifted parcels. *Wea. Forecasting,* **17,** 885–890.

Davies, J. M., 1993: Hourly helicity, instability, and EHI in forecasting supercell tornadoes. Preprints, *17th Conf. on Severe Local Storms,* St. Louis, MO, Amer. Meteor. Soc., 107–111.

——, 2004: Estimations of CIN and LFC associated with tornadic and nontornadic supercells. *Wea. Forecasting,* **19,** 714–726.

Davies-Jones, R. P., D. Burgess, and M. Foster, 1990: Test of helicity as a tornado forecast parameter. Preprints, *16th Conf. on Severe Local Storms,* Kananaskis Park, AB, Canada, Amer. Meteor. Soc., 588–592.

Dial, G. L., J. P. Racy, and R. L. Thompson, 2010: Short-term convective mode evolution along synoptic boundaries. *Wea. Forecasting,* **25,** 1430–1446.

Doswell, C. A., III, and D. M. Schultz, 2006: On the use of indices and parameters in forecasting severe storms. *Electron. J. Severe Storms Meteor.,* **1** (3). [Available online at http://www.ejssm.org/ojs/index.php/ejssm/issue/view/3.]

Esterheld, J. M., and D. J. Giuliano, 2008: Discriminating between tornadic and non-tornadic supercells: A new hodograph technique. *Electron. J. Severe Storms Meteor.,* **3** (2). [Available online at http://www.ejssm.org/ojs/index.php/ejssm/issue/view/13.]

Hart, J. A., and W. Korotky, 1991: The SHARP workstation v1.50 user's guide. National Weather Service, 30 pp. [Available from NWS Eastern Region Headquarters, 630 Johnson Ave., Bohemia, NY 11716.]

Maddox, R. A., L. R. Hoxit, and C. F. Chappell, 1980: A study of tornadic thunderstorm interactions with thermal boundaries. *Mon. Wea. Rev.,* **108,** 322–336.

Markowski, P. M., E. N. Rasmussen, and J. M. Straka, 1998: The occurrence of tornadoes in supercells interacting with boundaries during VORTEX-95. *Wea. Forecasting,* **13,** 852–859.

——, C. Hannon, J. Frame, E. Lancaster, A. Pietrycha, R. Edwards, and R. L. Thompson, 2003: Characteristics of vertical wind profiles near supercells obtained from the Rapid Update Cycle. *Wea. Forecasting,* **18,** 1262–1272.

Mason, I., 1982: A model assessment of weather forecasts. *Aust. Meteor. Mag.,* **30,** 291–303.

Miller, D. J., 2006: Observations of low level thermodynamic and wind shear profiles on significant tornado days. Preprints, *23rd Conf. on Severe Local Storms,* St. Louis, MO, Amer. Meteor. Soc., 3.1. [Available online at http://ams.confex.com/ams/pdfpapers/115403.pdf.]

NRC, 2006: *Completing the Forecast: Characterizing and Communicating Uncertainty for Better Decisions Using Weather and Climate Forecasts*. National Academies Press, 124 pp.

Rasmussen, E. N., 2003: Refined supercell and tornado parameters. *Wea. Forecasting,* **18,** 530–535.

——, and D. O. Blanchard, 1998: A baseline climatology of sounding-derived supercell and tornado forecast parameters. *Wea. Forecasting,* **13,** 1148–1164.

Schneider, R. S., and A. R. Dean, 2008: A comprehensive 5-year severe storm environment climatology for the continental United States. Preprints, *24th Conf. on Severe Local Storms,* Savannah, GA, Amer. Meteor. Soc., 16A.4. [Available online at http://ams.confex.com/ams/pdfpapers/141748.pdf.]

Stanski, H. R., L. J. Wilson, and W. R. Burrows, 1989: Survey of common verification methods in meteorology. World Weather Watch Tech. Rep. 8, WMO/TD 358, 114 pp.

Stensrud, D. J., J. V. Cortinas Jr., and H. E. Brooks, 1997: Discriminating between tornadic and nontornadic thunderstorms using mesoscale model output. *Wea. Forecasting,* **12,** 613–632.

Thompson, R. L., and R. Edwards, 2000: An overview of environmental conditions and forecast implications of the 3 May 1999 tornado outbreak. *Wea. Forecasting,* **15,** 682–699.

——, and C. M. Mead, 2006: Tornado failure modes in central and southern Great Plains severe thunderstorm episodes. Preprints, *23rd Conf. on Severe Local Storms,* St. Louis, MO, Amer. Meteor. Soc., 3.2. [Available online at http://ams.confex.com/ams/pdfpapers/115239.pdf.]

——, R. Edwards, J. A. Hart, K. L. Elmore, and P. M. Markowski, 2003: Close proximity soundings within supercell environments obtained from the Rapid Update Cycle. *Wea. Forecasting,* **18,** 1243–1261.

——, C. M. Mead, and R. Edwards, 2007: Effective storm-relative helicity and bulk shear in supercell thunderstorm environments. *Wea. Forecasting,* **22,** 102–115.

——, J. S. Grams, and J. A. Prentice, 2008: Synoptic environments and convective modes associated with significant tornadoes in the contiguous United States. Preprints, *24th Conf. Severe Local Storms,* Savannah, GA, 16A.3. [Available online at http://ams.confex.com/ams/pdfpapers/142210.pdf.]

——, R. Edwards, and C. M. Mead, cited 2011: An update to the supercell composite and significant tornado parameters. [Available online at http://ams.confex.com/ams/pdfpapers/82100.pdf.]

Wicker, L. J., 1996: The role of near surface wind shear on low-level mesocyclone generation and tornadoes. Preprints, *18th Conf. on Severe Local Storms,* San Francisco, CA, Amer. Meteor. Soc., 115–119.

Wilks, D. S., 2006: *Statistical Methods in the Atmospheric Science*. 2nd ed. Academic Press, 627 pp.